13TH CANADIAN MASONRY SYMPOSIUM
HALIFAX, CANADA
JUNE 4TH – JUNE 7TH 2017

INFLUENCE OF THE LOADING HISTORY ON THE IN-PLANE FORCE-DISPLACEMENT RESPONSE OF URM WALLS

Wilding, Bastian Valentin[1]; Dolatshahi, Kiarash[2] and Beyer, Katrin[3]

ABSTRACT

Quasi-static cyclic in-plane shear tests on unreinforced masonry (URM) walls are carried out to experimentally determine parameters that are of interest in the design process, e.g. effective stiffness, force capacity, drift capacity. Yet, the structural capacities can be a function of the demand and therefore dependent on the applied loading history. Although the effect of loading histories on URM wall capacities has not been investigated systematically, the comparison of few pairs of tests where monotonic and cyclic tests were performed indicated that in particular the drift capacities can be rather sensitive to the applied loading history. Structural design codes provide estimates of drift capacities that have been derived from sets of tests in which different loading protocols have been applied. Hence, an improved understanding of the influence that loading protocols can have on stiffness, shear force and drift capacities of URM walls would be important and would help reduce the uncertainties that are currently associated with the seismic assessment of URM buildings. This paper assesses the influence of the in-plane loading protocol on the force-displacement behaviour of unreinforced masonry walls by means of a numerical investigation. Four representative walls (two shear and two flexure controlled) from literature are modeled and subjected to several loading protocols. The occurring differences in effective stiffness, peak shear strength, energy dissipation as well as ultimate drift capacity are presented and discussed.

KEYWORDS: *unreinforced masonry wall, quasi-static cyclic test, displacement demand, displacement capacity, drift, load history, loading protocol*

INTRODUCTION

Displacement-based seismic design of in-plane loaded modern unreinforced masonry (URM) walls is based on several parameters to approximate the force-drift response by means of a bi-

[1] PhD Student, Earthquake Engineering and Structural Dynamics Laboratory (EESD), École Polytechnique Fédérale de Lausanne (EPFL), Lausanne, Vaud, Switzerland, bastian.wilding@epfl.ch
[2] Assistant Professor, Civil Engineering Department, Sharif University of Technology, Visiting Professor of the EESD-laboratory at EPFL, Lausanne, Vaud, Switzerland, dolatshahi@sharif.edu
[3] Assistant Professor and Head of the Earthquake Engineering and Structural Dynamics Laboratory (EESD), École Polytechnique Fédérale de Lausanne (EPFL), Lausanne, Vaud, Switzerland, katrin.beyer@epfl.ch

linear curve—drift is the horizontal displacement divided by the wall height. Necessary parameters are the effective stiffness, the peak shear strength as well as drift capacities of the wall. In most current codes, e.g. [1]–[4], the determination of the drift capacities is based on empirical models fitted to data of mainly quasi-static cyclic shear-compression tests of URM walls. These drift capacities, however, seem to depend on the seismic demand the wall is subjected to. Hence, the loading protocol employed in the tests influences the test results [5], [6].

Yet, the used loading protocols differ from testing campaign to testing campaign (e.g. [7]–[11]). Besides showing significant similarities (cyclically increasing, drift limit mean of zero) both the actual drift limits along with the number of cycles per drift limit can differ. This might be of concern, since all test results are evaluated together, notwithstanding of the exact loading protocol that was applied. Furthermore, there is a sheer abundance of suggested cyclic loading protocols for tests of different materials and structural applications to be found in literature: [6], [12]–[20] to name a few.

This paper investigates the influence of a change in seismic demand on characteristics of the force-horizontal displacement response of the URM wall, such as: effective stiffness, peak shear force, corresponding drift, ultimate drift capacity and energy dissipation. First, the rather scarce experimental evidence on using different loading protocols under otherwise similar kinematic and static boundary conditions in shear-compression tests of URM walls is presented. Subsequently, the seismic demand of different loading protocols in literature designed for or at least applicable to masonry shear wall tests is compared. Following, a numerical study is carried out simulating four wall tests (two shear and two flexure controlled) to be found in literature [10], [11] subjected to different loading protocols. Finally, the force-displacement responses are compared, interpreted and conclusions are drawn.

EXPERIMENTAL EVIDENCE

To the authors' knowledge, the sole evidence of pairs of URM walls tested with different loading protocols (monotonic vs. cyclically increasing) stems from campaigns by Ganz & Thürlimann [7] and Magenes & Calvi [23]. The tests indicated that while the effective stiffness and the peak shear strength of the walls remained more or less constant, notwithstanding the changing loading protocol, the ultimate drift capacity approximately doubled from cyclic to monotonic tests.

In an experimental campaign of reinforced masonry walls by Tomazevic et al [24] multiple identical specimens were subjected to different loading conditions: monotonic, cyclically increasing, cyclically increasing superimposed with additional sine function and simulated earthquake response. While both cyclic loading protocols were found to describe the dynamic tests with sufficient accuracy, the monotonic tests showed both significantly higher shear force capacities and ultimate drift capacities.

SEISMIC DEMAND OF LOADING PROTOCOLS IN LITERATURE

The cumulative drift demands of loading protocols to be found in literature are compared in Figure 1 by means of the sum of the drift limits δ_i up to a reference drift of 1 %. The considered protocols are: two loading protocols (MBL,H and P87 [6], [21]) explicitly designed for masonry, one widely used loading protocol (F461 [19]) without specification of the material to be used with, a loading protocol with a mean of the drift limits other than zero (K01 [22]), originally conceived for wood frame structures and further protocols used in testing campaigns (B04, B06, PB15, S15 [8]–[11]). There is a significant variation in seismic demand among the presented loading protocols. All the presented loading protocols used in testing campaigns impose a higher seismic demand as would be suggested for regions of low to moderate seismicity and even high seismicity regions according to [6].

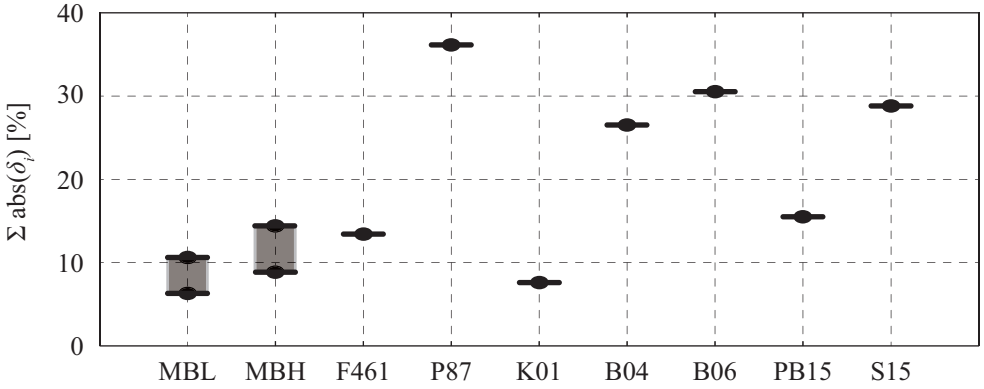

Figure 1: Comparison of seismic demand of loading protocols by means of the sum of the drift limits up to a reference drift limit of 1 % (MBL – [6] **full range of considered periods of structures for regions of low to moderate seismicity, MBH –** [6] **full range of considered periods of structures for high seismicity regions, F461 – FEMA461** [19]**, P87 – Porter** [21]**, K01 – Krawinkler et al** [15]**, B04 – test campaign by** [8]**, B06 – test campaign by** [9]**, PB15 – test campaign by** [11]**, S15 – test campaign by** [10]

ANALYSIS

A numerical study to assess the influence of different applied loading protocols on the force-displacement behaviour of the wall is conducted in the following. First, the tested walls to be simulated in the analysis are presented. Second, the numerical modeling approach is briefly introduced. Subsequently, the methodology of how to vary the loading protocols systematically to single out influencing parameters is described. Concluding the results of the analyses are presented, interpreted and conclusions are drawn.

Analysed wall tests

The analysed walls are from two experimental studies of the same masonry typology. The tests were performed as quasi-static cyclic shear-compression tests in which the axial load was kept constant and the walls were subjected to drift cycles of increasing amplitude. For the analysis two walls from each test campaign with identical geometry but subjected to different axial loads were chosen. The two specimens T1 and T3 from the test campaign by Salmanpour et al [10] were

subjected to double bending, showed diagonal shear cracking and failed in shear. T3 was tested under a higher axial load than T1. Specimens PUP3 and PUP4 by Petry & Beyer [11] were tested under a shear span of 1.5 times the wall height and exhibited rocking along with toe crushing. The only difference was, again, the axial load the walls were subjected two in the tests. The wall parameters are listed in Table 1.

Table 1: Chosen wall tests from literature to be used in the study

Name	L	H	H_0/H	h_B	l_B	σ_0	μ	c	f_u	$f_{B,c}$	E	δ_{ult}
	[mm]	[mm]	[-]	[mm]	[mm]	[MPa]	[-]	[MPa]	[MPa]	[MPa]	[MPa]	[%]
T1	2700	2600	0.50	190	290	0.58	0.48	0.26	5.80	26.3	3550	0.28
T3	2700	2600	0.50	190	290	1.16	0.48	0.26	5.80	26.3	3550	0.22
PUP3	2010	2250	1.50	190	300	1.05	0.94	0.27	5.86	35.0	3550	0.70
PUP4	2010	2250	1.50	190	300	1.54	0.94	0.27	5.86	35.0	3550	0.36

Numerical model

The walls are analysed on the finite element platform Abaqus 6.14 [25] using the modeling approach and a material subroutine by Aref & Dolatshahi [26]. The simulation is carried out as dynamic analysis with an explicit solution procedure.

The modeling approach is presented in more detail in [26] and is based on the works of Lourenco [28] as well as Oliviera et al [29]. In this 3D meso-scale modeling procedure, the bricks are expanded on each side by half the mortar joint width and are modelled as solid elements (C3D8R). Zero-thickness interface elements (COH3D8) are placed between the bricks representing the bed- and head-joints. Additionally, the same interface elements (COH3D8) are introduced vertically in the middle of each brick representing a possible fracture plane.

The material behaviour of the solid elements that represent the bricks is described with the 'Concrete Damaged Plasticity model', which is already implemented in Abaqus 6.14. This permits to explicitly simulate brick crushing. The behaviour of the interface elements follows the above-mentioned material subroutine, which is based on a plasticity model featuring an exponentially degrading yield surface in tension and shear. This approach allows for a simulation of bed-joint sliding and horizontal flexural cracking due to uplift in the bed-joints.

Validation of numerical model

To validate the numerical approach, the cyclically increasing loading protocols from the respective test campaign are applied on the considered walls. Figure 2 shows the shear force-drift curves from the respective test and the corresponding numerical simulation while Figure 3 shows the deformed shape per wall including the plastic equivalent strain distribution, which represents a measure for the occurring damage. As visible, there is a fairly good fit for all four considered walls including the deformed shapes that look reasonable for the respective wall behaviour types; diagonal cracking and damage within the whole wall area for shear dominated walls—Figure 3a, b—and rocking along with a concentration of the damage at the wall toe as can be seen in Figure 3c, d.

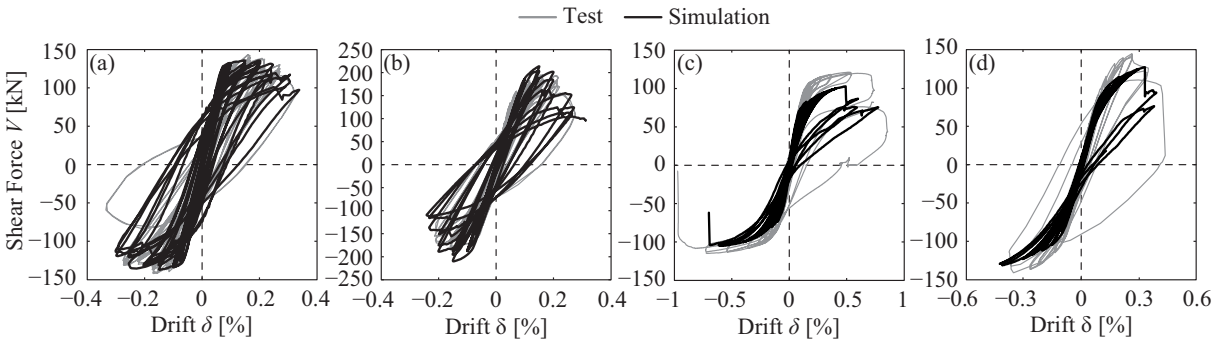

Figure 2: Shear force-drift curves of tests and numerical analysis, (a) T1 by [10]**, (b) T3 by** [10]**, (c) PUP3 by** [11]**, (d) PUP4 by** [11]

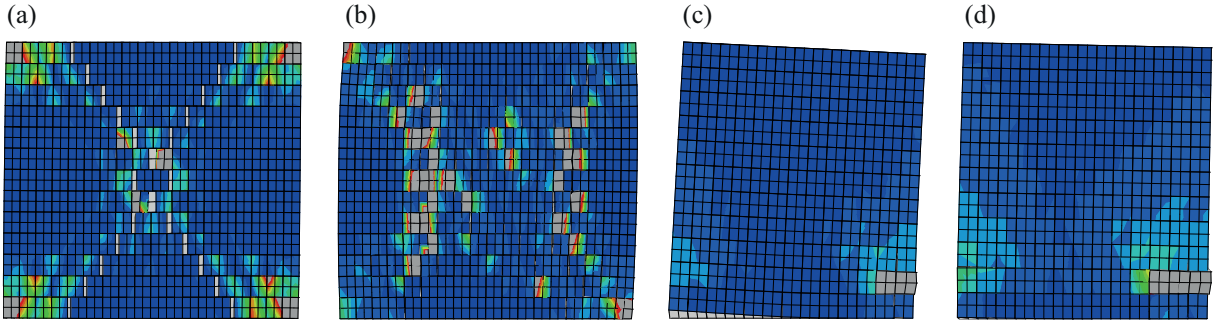

Figure 3: Corresponding deformed shape and plot of plastic equivalent strains near ultimate drift for (a) T1 by [10]**, (b) T3 by** [10]**, (c) PUP3 by** [11]**, (d) PUP4 by** [11]

Methodology

After the validation of the numerical model with the cyclic loading protocol from the tests, the loading protocols are varied in a systematic manner to isolate different influencing factors on the global load-displacement behaviour. The resulting set of loading protocols is shown in Table 2.

i. Monotonic loading
ii. Cyclically increasing loading protocols with drift limits (δ_i) according to FEMA 461 [19]
iii. Change of the number of cycles (n_1) per drift limit from one to three.
iv. Change of the mean of the drift limits $mean(\delta_i)$ (so far zero since reversed cyclically increasing) by using non-reversed cyclically increasing loading protocols with drift limits according to FEMA 461 [19].
v. Change of the number of cycles (n_1) per drift limit is changed for the non-reversed cyclic loading protocols.

Table 2: Set of cyclically increasing loading protocols used for each of the considered walls

Name	reference δ_i	n	n_1	mean δ_i [%]
Monotonic	-	1	1	0.50
F461NC1	FEMA 461 [19]	10	1	0.17
F461NC3		10	3	0.17
F461RC1		10	1	0
F461RC2		10	2	0
F461RC3		10	3	0
PB15RC2	Petry & Beyer [11]	11	2	0
S15RC3	Salmanpour et al. [10]	14	3	0

n ... number of different drift limits up to a reference drift of 1 %, n_1 … cycles per drift limit, mean δ_i calculated up to reference drift of 1 %

RESULTS

The results are presented and interpreted with regard to the following parameters: the peak shear capacity (V_P), the corresponding drift (δ_P), the effective stiffness (k_{ef})—the stiffness of the system at first attainment of 0.7 V_P, the ultimate drift capacity (δ_{ult})—the drift in the post-peak range at which the maximum attainable shear force drops below 0.8 V_P and the dissipated energy (ε_d) up to ultimate drift. The four considered walls were all subjected to the same set of loading protocols (see Table 2) while keeping all other boundary conditions constant.

Shear dominated walls

Figure 4 compares the shear force-drift envelops of the computed responses for the two considered shear dominated walls. Apparently, the ultimate drift capacities vary quite strongly depending on the used loading protocol. Monotonic loading leads to around twice as high a drift capacity than the reversed-cyclic loading protocol used in the test which seems to confirm experimental observations in [7] and [23]. Furthermore, the peak shear capacity is higher for monotonic than for cyclic loading. These observations hold true for both considered shear controlled walls.

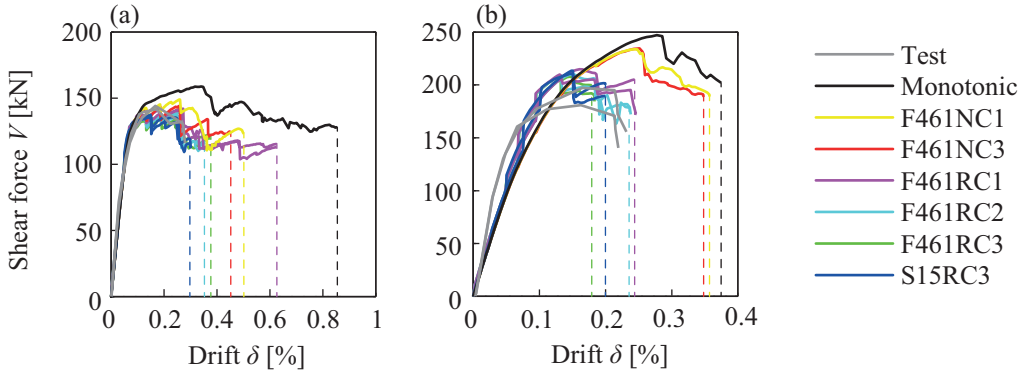

Figure 4: Envelops of shear force-drift responses as obtained in the test and simulations under different loading protocols including indication of attained ultimate drift in a simulation, (a) wall T1, (b) wall T3

A more detailed look on characteristic parameters can be obtained by comparing them in a normalised manner with respect to the used loading protocol which is done in Figure 5. Both the

ultimate drift capacity (δ_{ult}) and the drift at peak shear strength (δ_P) reduce significantly for non-monotonic loading protocols with the strongest decrease for the reversed-cyclic ones. Apparently, a change of the number of cycles (n_1) per drift limit does not influence the drift capacities as strongly, despite one outlier in Figure 5a: wall T1 subjected to loading protocol F461RC1. Here the shear force dropped rather late below the 0.8 V_P threshold but already approached it very closely around the ultimate drift capacities related to the loading protocols with a higher n_1.

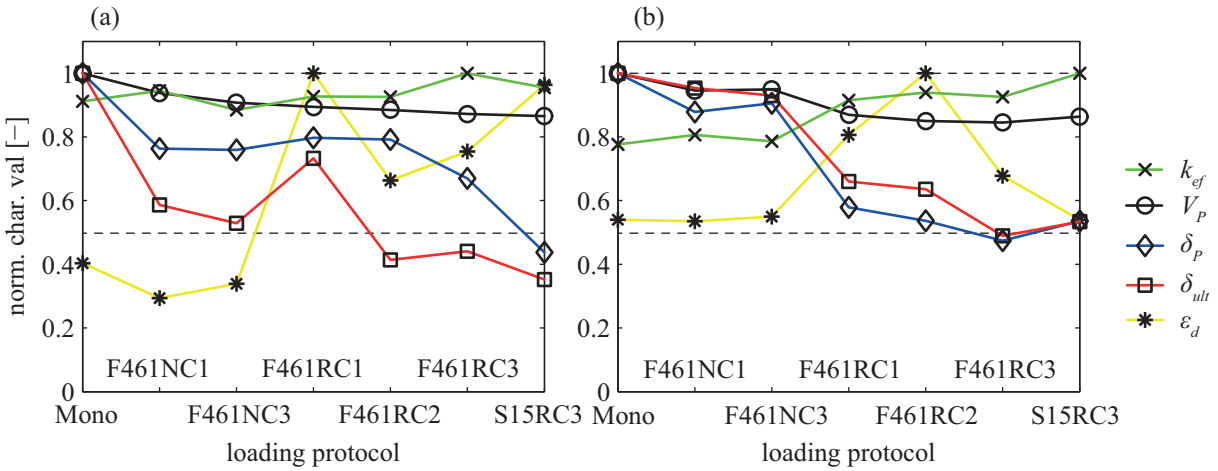

Figure 5: Trends in characteristic values (effective stiffness—k_{ef}, peak shear force capacity—V_P, corresponding drift—δ_P, ultimate drift—δ_{ult}) with changing loading protocols for (a) wall T1, (b) wall T3

It is also interesting to see that for a lower axial load—corresponding to wall T1, Figure 5a—the ultimate drift is already significantly lower for non-reversed cyclic loading protocols than in the monotonic case. Higher axial loads (wall T3 in Figure 5b), in contrast, seem to lead to comparable ultimate drift capacities for monotonic and non-reversed loading protocols and the drop to about 50 % of the monotonic drift capacity happens only for the reversed cyclic ones. The effective stiffness (k_{ef}) seems to generally show an increase from monotonic to reversed-cyclic loading and as for the shear force capacity (V_P), it shows the opposite trend: a decrease for an increase in seismic demand. Concerning the dissipated energy, the trend is less clear but ε_d seems to be rather constant for non-reversed (and monotonic) loading protocols. Furthermore, it is higher for reversed-cyclic loading protocols than for non-reversed ones.

Flexure dominated walls

The shear force-drift envelops of the flexure dominated walls subjected to different loading protocols are presented in Figure 6. Unlike for shear dominated walls, the scatter in ultimate drifts is significantly less pronounced hinting at a strongly reduced influence of the seismic demand on the force and drift capacities of the wall.

Figure 7 shows a more detailed insight, revealing that the effective stiffness and the dissipated energy increase for reversed-cyclic loading protocols. All the other parameters stay more or less constant notwithstanding the applied loading protocol.

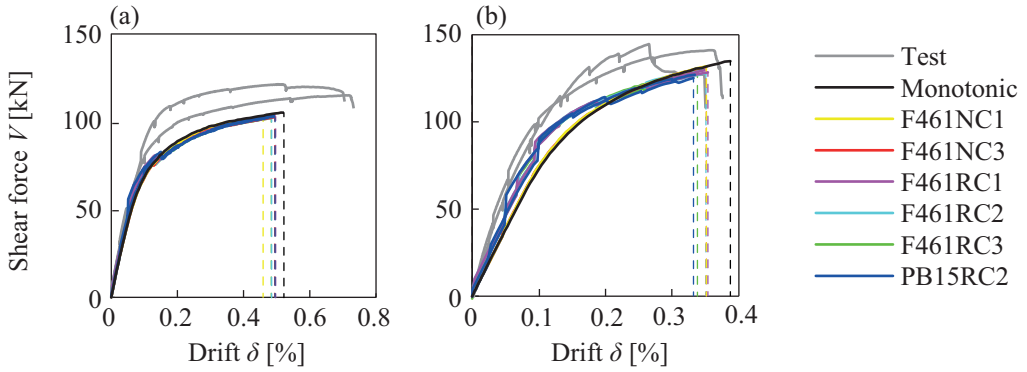

Figure 6: Envelops of shear force-drift responses as obtained in the test and simulations under different loading protocols including indication of attained ultimate drift in a simulation, (a) wall PUP3, (b) wall PUP4

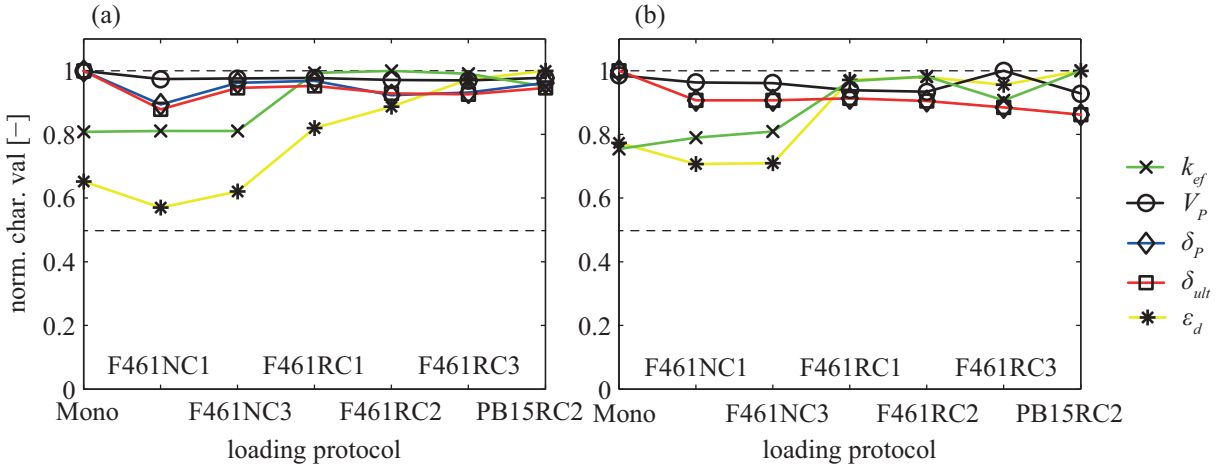

Figure 7: Trends in characteristic values (effective stiffness—k_{ef}, peak shear force capacity—V_P, corresponding drift—δ_P, ultimate drift—δ_{ult}) with changing loading protocols for (a) wall PUP3, (b) wall PUP4

Discussion of results

One explanation for the difference between shear and flexure dominated walls concerning the influence of the seismic demand on the wall force and drift capacities could be the impact of localized damage. In shear controlled walls, large parts of the wall show damage (see Figure 3a, b) and, hence, contribute to the wall capacity. The lower the seismic demand, the lower the overall damage, e.g. monotonic loading will only damage approximately half of the wall area than cyclic loading will. As a consequence, the higher the overall damage, the lower are the drift and shear force capacities. The characteristic parameters in flexure dominated walls (drift and force capacity), however, are dependent on a more localized concentrated zone around the wall toe (as can be seen in Figure 3c, d). Hence, as soon as there is failure in this zone, the wall shows ultimate failure which significantly reduces its susceptibility to a change in seismic demand.

It seems that cyclically increasing loading protocols with rather high seismic demands—that are usually used—are a safe and conservative way of testing. The number of cycles (n_1) per drift limit

seems not to be very significant. The important aspect is the drift limit mean, with a mean of zero (e.g. reversed cyclic loading) imposing maximum damage and, hence, causing the lowest drift capacities. However, apparently shear dominated walls can support higher drifts if they are loaded in a non-reversed manner which might happen for structural elements in real earthquake conditions due to the ratcheting effect [5].

However, the presented results are only based on a limited number of simulations of certain wall configurations. The observed trends strictly apply for a wall aspect ratio of around one—the aspect ratio of the simulated walls. As mentioned, the effect of the load history on force and drift capacity depends mainly on the damage pattern, which might be different for other wall aspect ratios. Furthermore, only one masonry typology was considered in this study; walls with vertically perforated clay units, normal strength mortar (compressive strength of 5 to 10MPa) and bed-joints of normal thickness (~1cm). Therefore, the presented study should be regarded as a preliminary research approach that provides first indications on the influence of the load history on the wall force-displacement behaviour. It is, moreover, suggested to validate the identified trends with an extensive experimental campaign.

CONCLUSIONS

This article investigates the influence of the seismic demand on the capacity of URM walls loaded in-plane by means of a numerical study. Four walls tested in literature (two shear dominated and two flexure controlled) are simulated and subjected to different loading protocols.

Shear dominated walls show a rather strong dependency of ultimate drift and drift at peak strength on the seismic demand—the drift capacity for reversed-cyclic loading can be up to 50 % lower than for monotonic loading. Furthermore, a negative trend for peak shear capacity vs seismic demand and a positive one for the effective stiffness can be observed. Generally it seems that the number of cycles per drift limit does not have that much of an influence on effective stiffness, strength and deformation capacity of the walls but rather the loading protocol mean, with a mean of zero—reversed-cyclic loading protocols—leading to the most conservative results. It seems that cyclically increasing loading protocols with rather high seismic demands—that are usually used—are a safe and conservative way of testing. The testing in a reversed manner achieves maximum damage in the shear controlled wall and, hence, yields a conservative estimate of peak shear strength and drift capacities.

The force-displacement behaviour of flexure dominated walls, on the contrary, appears not to be sensitive to a change in seismic demand apart from an increasing effective stiffness between non-reversed and reversed cyclic loading protocols. Hence, for flexure controlled walls, monotonic tests might be sufficient to obtain the parameters necessary for seismic design.

The presented results are based on numerical simulations. An experimental campaign that explicitly investigates the influence of the seismic demand on stiffness, force and drift capacities of unreinforced masonry walls should, therefore, be carried out to validate the identified trends.

ACKNOWLEDGEMENT

This study was supported by the grant no. 159882 of the Swiss National Science Foundation: "A drift capacity model for unreinforced masonry walls failing in shear".

REFERENCES

[1] CEN, "EN 1998-3: 2005 Eurocode 8: Design of structures for earthquake resistance - Part 3: Assessment and retrofitting of buildings," Comité Européen de Normalisation, 2005.

[2] NTC, "Decreto Ministeriale 14/1/2008: Norme tecniche per le costruzioni," Ministry of Infrastructures and Transportations, 2008.

[3] ASCE, "FEMA 356 - Prestandard and Commentary for the Seismic Rehabilitation of Buildings," American Society of Civil Engineers, Reston, Virginia, 2000.

[4] NZSEE, "Assessment and Improvement of Unreinforced Masonry Buildings for Earthquake Resistance, New Zealand Society of Earthquake Engineering, supplement to 'Assessment and improvement of the structural performance of buildings in earthquakes,'" University of Auckland, 2011.

[5] H. Krawinkler, "Loading histories for cyclic tests in support of performance assessment of structural components," *3AESE Conf. (3rd Int. Conf. Adv. Exp. Struct. Eng.*, pp. 1–10, 2009.

[6] P. Mergos and K. Beyer, "Loading protocols for European regions of low to moderate seismicity," *Bull. Earthq. Eng.*, vol. 504, no. 12, pp. 2507–2530, 2014.

[7] H. Ganz and B. Thürlimann, "Versuche an Mauerwerksscheiben unter Normalkraft und Querkraft," Test Report, ETH Zürich, 1984.

[8] V. Bosiljkov, M. Tomazevic, and M. Lutman, "Optimization of shape of masonry units and technology of construction for earthquake resistant masonry buildings - Part One and Two," Lubljana, Slowenia, 2004.

[9] V. Bosiljkov, M. Tomazevic, and M. Lutman, "Optimization of shape of masonry units and technology of construction for earthquake resistant masonry buildings - Part Three," Lubljana, Slovenia, 2006.

[10] A. H. Salmanpour, N. Mojsilović, and J. Schwartz, "Displacement capacity of contemporary unreinforced masonry walls: An experimental study," *Eng. Struct.*, vol. 89, pp. 1–16, Apr. 2015.

[11] S. Petry and K. Beyer, "Cyclic Test Data of Six Unreinforced Masonry Walls with Different Boundary Conditions," *Earthq. Spectra*, vol. 31, no. 4, pp. 2459–2484, Nov. 2015.

[12] ATC, "ATC 24: Guidelines for cyclic seismic testing of components of steel structures," Applied Technology Council (ATC), Washington DC, 1992.

[13] R. Behr and A. Belarbi, "Seismic test methods for architectural glazing systems," *Earthq. Spectra*, vol. 12, no. 1, 1996.

[14] P. Clark, K. Frank, H. Krawinkler, and R. Shaw, "Protocol for fabrication, inspection, testing and documentation of beam-column connection tests and other experimental specimens," 1997.

[15] H. Krawinkler, F. Parisi, L. Ibarra, A. Ayoub, and R. Medina, "Development of a testing protocol for woodframe structures," CUREE, publication No. W-02, 2001.

[16] CEN, "EN 12512 Cyclic testing of joints made with mechanical fasteners," Comité Européen de Normalisation, 2001.

[17] AISC, "ANSI/AISC 341-05 Seismic Provisions for Structural Steel Buildings," American Institute of Steel Construction, 2005.

[18] P. W. Richards and C. Uang, "Testing Protocol for Short Links in Eccentrically Braced

Frames," *J. Earthq. Eng.*, vol. 132, no. 8, pp. 1183–1191, 2006.
[19] ATC, "FEMA 461: Interim Testing Protocols for Determining the Seismic Performance Characteristics of Structural and Nonstructural Components," Applied Technology Council (ATC), Washington DC, 2007.
[20] R. Retamales, G. Mosqueda, A. Filiatrault, and A. Reinhorn, "Testing Protocol for Experimental Seismic Qualification of Distributed Nonstructural Systems," *Earthq. Spectra*, vol. 27, no. 3, pp. 835–856, 2011.
[21] M. L. Porter, "Sequential phased displacement (SPD) procedure for TCCMAR testing.," In: 3rd meeting of the joint technical coordinating committee on masonry research, US-Japan coordinated program, 1987.
[22] H. Krawinkler, A. Gupta, R. Medina, and N. Luco, "Development of loading histories for testing of steel beam to column assemblies," SAC Background Report, SAC/BD-00/10, 2000.
[23] G. Magenes and G. M. Calvi, "Cyclic behaviour of brick masonry walls," *Earthq. Eng. Tenth World Conf. Rotterdam*, 1992.
[24] M. Tomazevic, M. Lutman, and L. Petkovic, "Seismic behavior of masonry walls: experimental simulation," *J. Struct. Eng.*, vol. 122, no. 9, pp. 1040–1047, 1996.
[25] Dassault Systèmes, "Abaqus 6.14 Documentation," Dassault Systèmes Simulia Corp., Providence, RI, USA, 2014.
[26] A. J. Aref and K. M. Dolatshahi, "A three-dimensional cyclic meso-scale numerical procedure for simulation of unreinforced masonry structures," *Comput. Struct.*, vol. 120, pp. 9–23, 2013.
[27] Intel Corporation, "Intel ® Fortran Compiler 16.0 User and Reference Guide," 2015.
[28] P. B. Lourenço, "Computational strategies for masonry structures," PhD-Thesis, TU Delft, 1996.
[29] D. V. Oliveira, P. B. Lourenço, and P. Roca, "Cyclic behaviour of stone and brick masonry under uniaxial compressive loading," *Mater. Struct.*, vol. 39, no. 2, pp. 247–257, 2007.